



Variability of Dayside High Latitude Convection Associated with a Sequence of Auroral Transients

J. Moen,¹ M. Lockwood,² P.E. Sandholt,³ U.P. Løvhaug,⁴ W.F. Denig,⁵ A.P. van Eyken,⁴ and A. Egeland³

¹The University courses on Svalbard, Box 156, N-9170 Longyearbyen, Svalbard; ²Rutherford Appleton Laboratory, Chilton, Didcot, OX11 0QX, UK; ³Department of Physics, University of Oslo, Box 1048 Blindern, N-0316, Norway; ⁴EISCAT Scientific Association, Ramfjordmoen, N-9027 Ramfjordbotn, Norway; ⁵Phillips Laboratory, Geophysics Directorate, Hanscom APE, MA 01731, USA

(Received 27 October 1994; accepted in revised form 12 December 1994)

Abstract—10 second resolution ionospheric convection data covering the invariant latitude range from 71° to 76°, obtained by using the EISCAT UHF and VHF radars, are combined with optical data from Ny Ålesund during a sequence of auroral transients in the post-noon sector (~15 MLT). Satellite observations of polar cap convection patterns suggest negative B_z and B_y components of the interplanetary magnetic field. Burst-like enhancements of westward (sunward) post-noon convection were accompanied by eastward moving auroral forms at higher latitudes, above the convection reversal boundary. In this case the background convection was weak, whereas the integrated potential drop across the radar field-of-view associated with the westward flow bursts was typically ~20–35 kV. The auroral phenomenon consists of a series of similar events with a mean repetition period of 8 min. A close correlation between the auroral activity and convection enhancements in the cleft ionosphere is demonstrated.

1. INTRODUCTION

Studies of ionospheric transients in the cusp/cleft ionosphere are of particular interest since they may provide important information about the energy and momentum transfer from the solar wind into the magnetosphere through the dayside magnetopause, and hence elucidate the convection driver mechanism(s). The role of transient solar wind-magnetosphere coupling modes as convection drivers is not clear at present. Lockwood *et al.* (1989) reported a series of intermittent transient flow enhancements observed by EISCAT, each with a transitory auroral event termed 'midday auroral breakup' by Sandholt *et al.* (1989). This category of events occurs preferentially during periods of southward directed interplanetary magnetic field (IMF) and was interpreted as ionospheric footprints of flux transfer events (FTEs), in that the flow burst was described as arising from the tension force associated with the IMF B_y on the patch of newly-opened flux produced by a burst of reconnection at the dayside magnetopause.

Different modes of solar wind-magnetosphere interactions are expected to set up characteristic convection signatures in the ionosphere. Friis-Christensen *et al.* (1988) and Sibeck (1990) proposed that dynamic pressure variations at the magnetopause may excite

travelling convection vortices (TCVs) in the ionosphere-magnetosphere system. Kivelson and Southwood (1990) argued that a single pressure pulse creates a pair of oppositely rotating vortices associated with a pair of oppositely directed Birkeland currents. McHenry *et al.*, 1990a, McHenry *et al.*, 1990b) identified a continuous chain of TCVs located near the convection reversal boundary on field lines mapping to the inner edge of the low-latitude boundary layer and suggested that these vortices are signatures of the Kelvin-Helmholtz instability. However, Friis-Christensen *et al.* (1988) also pointed out that an observed change in the IMF orientation, may have produced the TCV they described, possibly by moving the site of dayside reconnection.

Several models of ionospheric flow signatures associated with FTEs have been proposed. A frequently used description of FTE flow excitation is the "moving cloud" model equivalent to the flow around a cylinder of circular or elliptical cross section moving in the ambient ionospheric plasma (e.g. Southwood, 1987; Lockwood *et al.*, 1990a; Wei and Lee, 1990). The principal idea behind these models is that the flow inside the flux rope is uniform, and that the surrounding ionospheric plasma (incompressible) is set into a localised twin-vortical motion as the path of the faster moving flux tube is pushed out. Wei

and Lee (1990) pointed out that an elongated plasma cloud, and hence a twin-vortex convection pattern, may originate from an impulsive plasma penetration event (PTE) as well. While vortices generated by pressure pulses or the Kelvin–Helmholtz instability propagate along the line combining the Birkeland current pair, FTE and PTE flow vortices move perpendicular to this line.

Cowley and Lockwood (1992) recently proposed a model for large-scale flow excitation due to time varying reconnection based on the concept of zero-flow equilibrium configurations of the magnetosphere which have an arbitrary amount of open flux, a work inspired by the theoretical convection model of Siscoe and Huang (1985) and the explanation of ionospheric effects of magnetospheric erosion by Freeman and Southwood (1988) (cf. also Lockwood *et al.*, 1990b). During southward IMF conditions the effect of impulsive reconnection at the magnetopause is to increase the amount of open flux in the magnetosphere. A two-cell convection pattern (strongest in the dayside ionosphere) is then excited to move the system back towards a new equilibrium state, in which the polar cap has expanded. The asymmetry of flow cells related to the IMF B_Y is expected to be as for continuous reconnection. In contrast to the Southwood (1987) model, where an FTE footprint, creates a moving small-scale flow distortion of minor importance for the large-scale polar cap convection, the Cowley and Lockwood (1992) model proposes that pulsed reconnection drives time varying Dungey cell convection and contributes significantly to the cross polar potential drop.

In this paper we present radar observations of bursty sunward flow enhancements at the equatorward side of a sequence of auroral transients in the post-noon sector (~ 15 MLT) on 7 January 1992. The optical observations are made from Ny Ålesund, Svalbard. Lockwood *et al.* (1993) have analysed combined optical and radar measurements taken about one hour and a half earlier on the same day. During their period of observations, a strongly enhanced plasma convection and the onset of dayside auroral transients followed a sudden equatorward motion of the 630.0 nm arc. These observations were found to be consistent with the expected effects of a southward turning of the IMF and associated time varying reconnection at the dayside magnetopause. After this sudden onset of activity at 1040 UT, a long sequence of similar ionospheric transients lasted until 1400 UT (~ 17 MLT). The time interval from 1145 to 1230 UT has been selected for this study.

The observations presented below reveal a close relationship between optical transients and variations

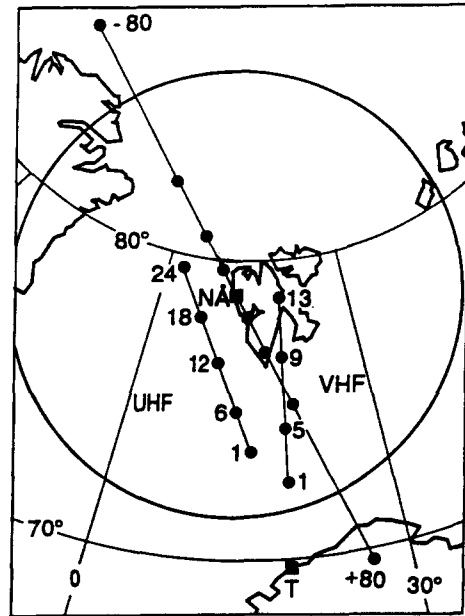


Fig. 1. Map showing the EISCAT UHF and VHF radar beams employed by the 5P-UK-CONV experiment. The numbered dots mark the range gate centres. The straight line through Ny Ålesund (NÅ) shows the meridian scanned by the 630.0 nm photometer, onto which dots indicate the locations of 20° steps in zenith angle, assuming an emission altitude of 300 km. The circle with the centre at Ny Ålesund marks the all-sky camera coverage.

of dayside convection. In this case there is little other source of flows and the extremely weak background convection allows us to quantify the potential likely to be associated with dayside auroral transients.

2. OBSERVATIONS

In this work we present ionospheric flow measurements with 10 sec resolution obtained by the EISCAT radars during a sequence of auroral transients. The auroral activity was monitored from Ny Ålesund by a Meridian Scanning Photometer (MSP) and an all-sky TV camera. Both the instruments were fitted by 630.0 nm filters. Ny Ålesund is located at 76° invariant latitude (ILAT) and crosses magnetic noon at ~ 0850 UT. The MSP has a 2° field-of-view and scans along the magnetic meridian to 10° above the northern and southern horizons, with a scan period of 18 sec. Fig. 1 shows the MSP scanning direction and geomagnetic latitudinal coverage assuming an altitude of 300 km for F-layer auroral emissions. The circle, with its centre at Ny Ålesund, indicates roughly the useful field-of-view of the all-sky camera. The EISCAT UHF and VHF radars were operated simultaneously in the SP-

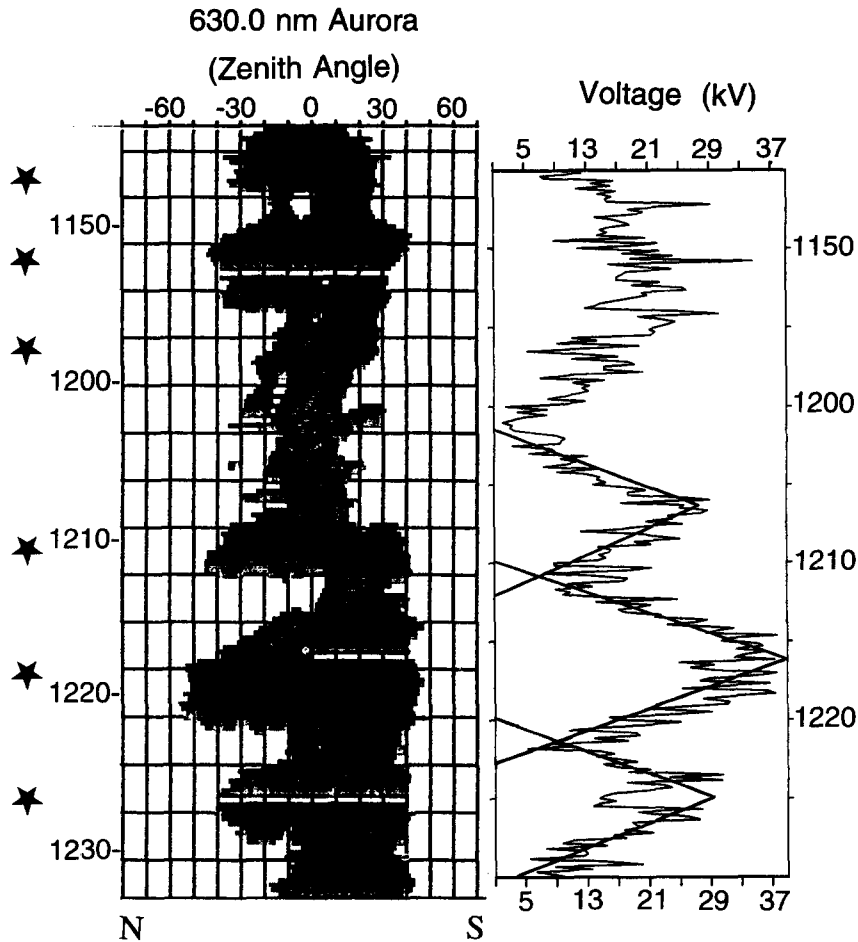


Fig. 2. (left) Location in zenith angle of the 630.0 nm aurora. The black dots within the grey belt mark intensity maxima. (right) Voltage (V) across the radar field-of-view (71° – 76° ILAT). The straight lines drawn indicate a linear approximation of growth and decay rates of flow voltage in response to a series of transitory momentum transfer (see text for details).

UK-CONV experiment mode. The UHF radar was pointing 160° west of geographical north at an elevation of 200° . The VHF beam was pointing 150° to the east of the UHF and at the lowest possible elevation of 300° (cf. Fig. 1). Assuming the ion flow to be constant along the L-shell, ion flow vectors at 17 adjacent gates covering the latitudinal range 71° – 76° ILAT are obtained by combining line-of-sight velocities measured by the two radars.

The left panel of Fig. 2 shows the MSP observations for the interval from 1145 to 1232 UT on January 07, 1992. Vertical lines mark each tenth degree zenith angle. North is to the left. The grey belt marks the location in zenith angle of the 630.0 nm luminosity and the black dots mark intensity maxima. A series of 6 auroral events, indicated by stars, appear as tran-

sient intensifications at the poleward side of the luminous background arc. From all-sky imaging we know that these auroral transients actually were eastward moving auroral forms traversing the scanning meridian. Fig. 3 shows a sequence of digitized all-sky camera images for the interval 1223–1228 UT. The dynamic colour scale given at the bottom left of the figure represents increasing intensity from left to right. The auroral emission at 630.0 nm is projected to an altitude of 300 km. Each of the 6 images represents an average of 1.28 sec video-recording starting at the time indicated on each frame. This sequence of images illustrates east and poleward motion of the last event occurring in Fig. 2. An auroral form, likely formed outside the camera field-of-view closer to noon, propagated/expanded from west to east at the pole-

ward side of the more persistent background arc. This auroral form is first defined in the image shown for 1223 UT on the western limb of the field-of-view, over the east coast of Greenland and its leading (eastern) edge reached the Ny Ålesund meridian by 1224 UT (second image) and hence was also detected by the MSP (cf. Fig. 2). In the subsequent images we observe the leading edge to remain close to the Ny Ålesund meridian and the event fades and shrinks as the trailing edge continues to propagate east, appearing as a faint patch north west of Svalbard by 1225 UT. A sequence of 15 similar events occurred within the two hours from 1130 UT to 1330 UT, which gives an average repetition period of ~ 8 minutes. These auroral forms were typically fading out at the Ny Ålesund meridian or slightly to the east of it.

The 557.7 nm MSP channel (not presented) shows that the auroral transient forms and the background cleft luminosity at lower latitudes had significantly different spectral characteristics. The transient forms were red-dominated while the background luminosity also included a strong 557.7 nm component.

Fig. 4 shows the ion flow vectors as function of time and invariant latitude during the time interval from 1200 to 1230 UT including three major convection events (for clarity, only every other 10 sec resolution flow vector has been plotted). The flow direction is relatively stable and pointing north-westward. Flow speeds $\sim 2\text{--}3\text{ km s}^{-1}$ occurred at the times of the major auroral events. Note that the eastward moving optical features were observed poleward of Ny Ålesund zenith and hence to the north of the poleward limit of the combined radar observations (UHF gate 17 and VHF gate 13 corresponding to 76° ILAT). In order to quantify the total westward flow (v_w) the voltage (V) across the radar field-of-view is estimated from $V = \sum_n v_w B_i dl$, where the sum is over all $n = 17$ gates (covering the range of invariant latitudes from 71° to 76° ILAT), B_i is the local magnetic field and dl is the distance between L shells of adjacent gates (≈ 35 km). The right panel of Fig. 2 shows the flow voltage (V) across the radar field-of-view as function of time. Note that the time scales on the MSP and the Voltage plots have been offset by 110 sec accounting for the mean radiative lifetime of the OI 1D state. The sequence of auroral activity is apparently correlated with major enhancements in flow voltage (up to 35 kV). Allowing for the excitation state lifetime of 110 sec, the flow voltage starts rising about 2 min before the onset of each major optical event. Times of maximum flow voltage are indicated by arrows in Fig. 4.

Fig. 5 shows DMSP-F11 measurements of the cross-track component of plasma drifts and the derived distribution of polar cap voltage obtained dur-

ing two successive northern and southern dawn-dusk passes within the time intervals 1125–1151 UT and 1217–1243 UT, respectively. The DMSP values of voltage, derived from the cross-track component of drift only, are underestimates of the total cross polar cap potential since the satellite orbits do not necessarily go through the potential maxima and minima. In this case the satellite flew close to the dawn–dusk meridian and the obtained values are assumed to be reasonably good estimates of the total transpolar voltage (Heppner and Maynard, 1987). The southern pass appears to be an encounter of the type BC pattern of Heppner and Maynard (1987). A striking feature of the northern pass is the well-defined evening cell convection with the sharp reversal boundary at 76° ILAT. The actual observation fits with the crescent shaped dusk cell and the more extensive morning cell of the type DE pattern of Heppner and Maynard (1987). The BC and DE type convection patterns in the southern and northern hemispheres, respectively, are characteristic of prevailing southward directed IMF ($B_z < 0$) with a negative B_y component. The transpolar voltage obtained by F11 during the northern and southern passes were 39 and 52 kV, respectively. Such relatively low polar cap potential values suggest that IMF $|B_z|$ was small during the actual time period (Doyle and Burke, 1983). The dominant dusk flow cell gave trans-auroral voltages of 30 kV and 45 kV, mainly over about 100 of invariant latitude (roughly twice the width of the EISCAT field-of-view). The evening cell flow reversal observed by F11 was located approximately at the poleward limit of the EISCAT field-of-view ($\sim 76^\circ$ ILAT). The moving auroral forms were located at latitudes poleward of the flow reversal boundary and hence on eastward convecting field lines.

3. DISCUSSION

The quasi-periodic sequence of 630.0 nm auroral forms moving along the polar cap boundary appears to be a most commonly observed event scenario during intervals of southward pointing IMF conditions. The aurora] transients described by Sandholt and his coworkers (e.g. Sandholt *et al.*, 1986; Sandholt *et al.*, 1989; Sandholt *et al.*, 1993) are characterized by brightening within the persistent cusp/cleft aurora. Subsequently they move in both the poleward and east–west directions detaching from the background arc. The east–west component of their motion is controlled by the IMF B_y . The events characteristically recur on a time scale of ~ 8 min. This auroral phenomenon is regarded as a possible footprint of pulsed



Fig. 3. Digitized all-sky 630.0 nm TV camera images from Ny Ålesund mapped onto a geographical frame of reference (for an assumed emission altitude of 300 km) for the time period interval 1223–1228 UT. The images are limited by the 700 zenith angle outside which the camera sensitivity falls rapidly. The dynamic synthetic colour scale was set to the most intense auroral feature within the sequence.

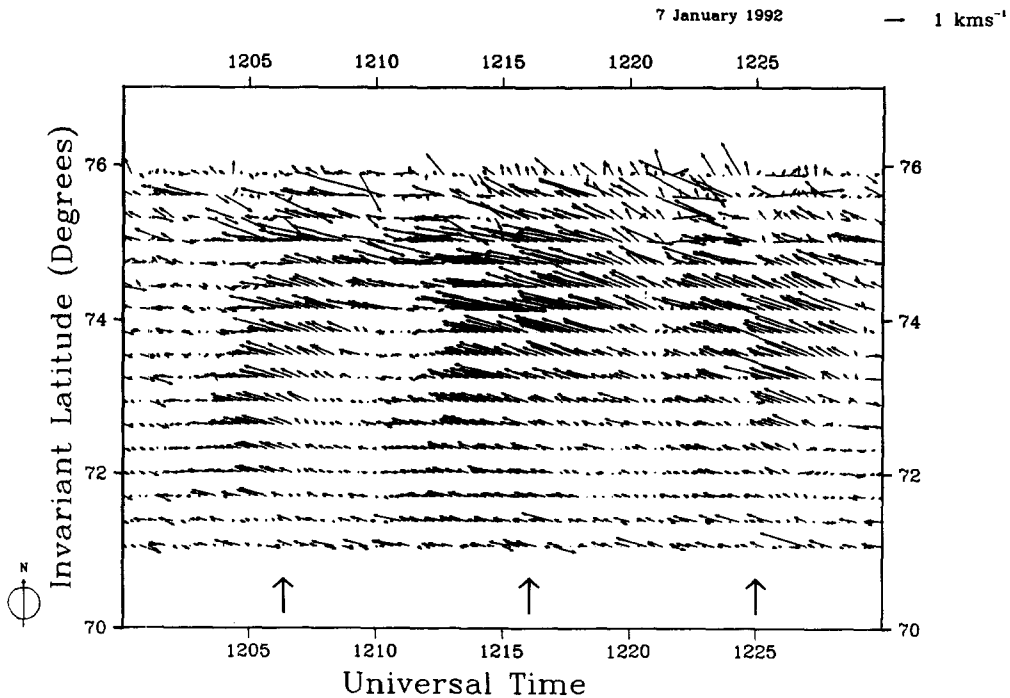


Fig. 4. Ion drift vectors at 17 range gates covering 71° – 76° ILAT obtained by operating the EISCAT UHF and VHF radars simultaneously in the SP-UK-CONV mode. The arrows below the flow vectors mark the times maxima in flow voltage.

reconnection at the magnetopause (flux transfer events, FTEs; Russell and Elphic, 1979). During intervals when the B_y and B_z components of the IMF are both negative, as inferred here, auroral activity related to reconnection is expected in the post-noon sector (cf. Sandholt *et al.*, 1993). The auroral forms reported here do not show the poleward component of motion in the fading phase which is a characteristic feature of auroral events that have been discussed as a possible FTE signature.

However, alternative explanations to FTEs have been discussed. Sibeck (1990) proposed that quasi-periodic solar wind/magnetosheath pressure pulses may trigger auroral events with similar features as those related to FTEs. Kelvin–Helmholtz instabilities (Wei and Lee, 1993) and impulsive plasma transfer events on closed field lines (PTEs; Woch and Lundin, 1992), are also expected to create auroral bursts in the dayside auroral ionosphere. PTEs appear as an interesting possibility, as the occurrence probability of filamentary plasma injections into the tail flanks maximizes around 16 MLT in the afternoon sector (Woch and Lundin, 1992). Plasma injections into the tail flanks do preferentially occur when the IMF is radially directed. Using ideal MHD (2-dimensional),

it has been shown that the magnetic field inside the magnetosheath plasma filament has to be strictly aligned with (parallel or antiparallel) the Earth's field for a penetration event to occur (Lemaire *et al.*, 1979; Ma *et al.*, 1991). Unfortunately, for the actual case we do not know the IMF orientation. Recently, Newell and Sibeck (1993) have proposed that the events are newly-reconnected field lines but reflect an increase in magnetosheath B_y for steady magnetopause reconnection.

Now let us consider the ionospheric flow measurements. The UHF and VHF radar beams were both located within the sunward convecting part of the dusk cell, i.e. equatorward of the convection reversal boundary. Since the poleward limit of the EISCAT field-of-view was located close to the convection reversal, the EISCAT flow voltage quantifies the sunward flow across the ~ 15 MLT meridian. From Fig. 2 we note several interesting features. The first three events (5 min repetition period) are associated with basically one flow enhancement peaking at ~ 20 kV. The convection then decayed to zero between events 3 and 4 (about 12 min apart). Furthermore the last three convection bursts were apparently correlated with successive auroral transients 8 min apart. The evi-

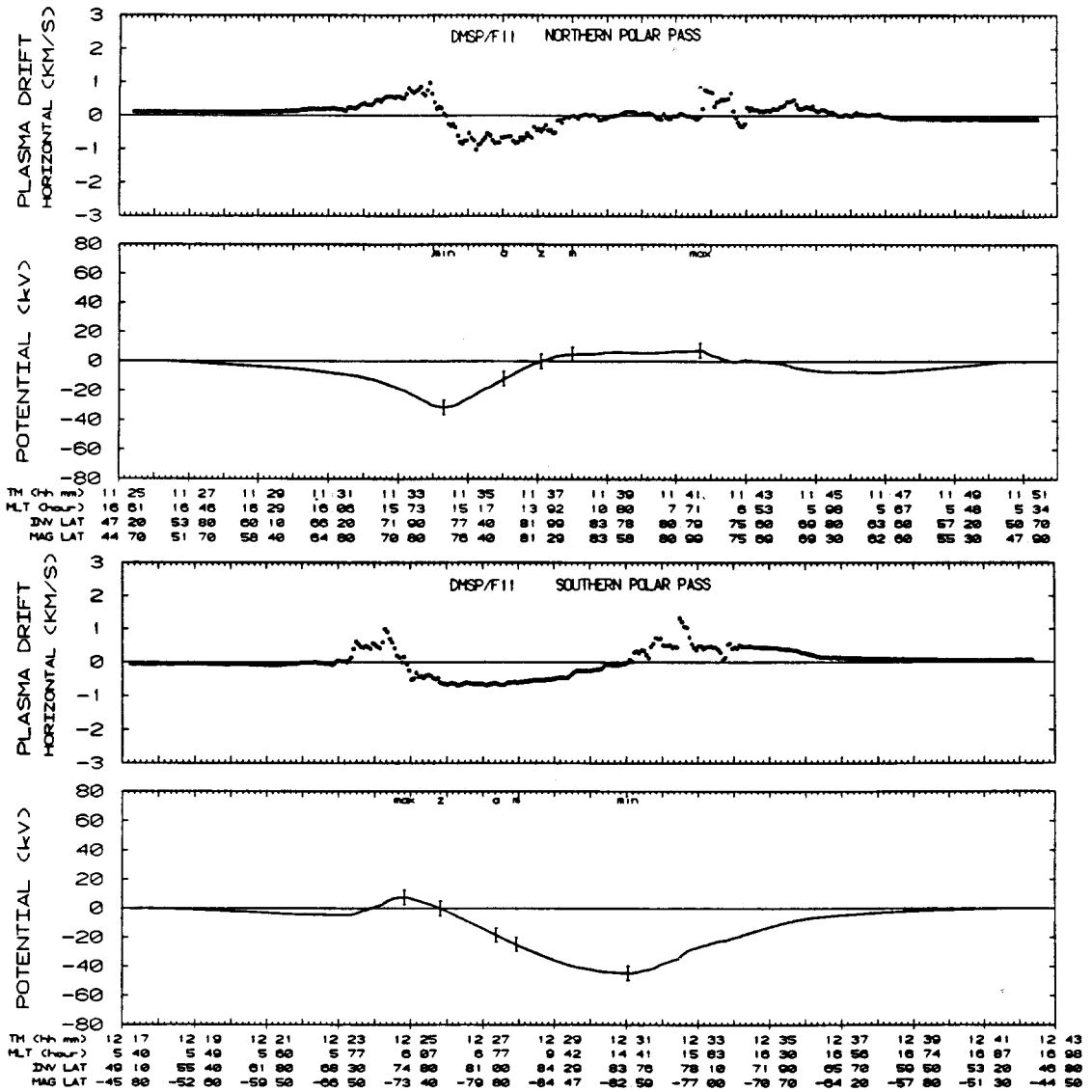


Fig. 5. F11 cross-track component of plasma flow and the derived total potential variation within the northern (NORTH) and southern (SOUTH) hemisphere passes during the intervals 1125–1151 UT and 1217–1243 UT, respectively. Positive (negative) sign of the drift plots indicates that plasma has a sunward (anti-sunward) component of flow.

dence that the flow voltage dropped to zero between events 3 and 4 is taken as an indicator of an extremely weak background convection.

From the EISCAT flow measurements only, it is not trivial to distinguish between flow variations caused by a small-scale flow pattern propagating through the radar beams, and/or temporary variation of large-scale flows. Let us first consider the possibility that the burst-like flow enhancements were caused by

a train of FTE/PTE magnetic flux ropes being pulled through the ionosphere from west to east. To make way for the faster moving flux tube, the ambient plasma (incompressible) is set into a localised double vortex flow pattern (cf. Introduction). According to a “moving cloud” model, each of the transient auroral forms is attributed to the cross section of the individual flux ropes. Hence, EISCAT could only be sampling the westward return flow set up equatorward of

the flux tubes. EISCAT was viewing at most one quarter of successive double vortex flow patterns passing by. As the flow bursts was located within the latitude interval from 72.5° to 75.5° ILAT, a scale size of ~ 1300 km is estimated for a double vortex system. The east–west extension of a flow pattern moving across the radar beams equals the time it took it to pass times the travelling speed of the event. Since the steady state background flow was minor, the travelling speed of the flux rope must be of the same order as the return flow speed. A typical flow burst with a speed of 2.5 km s^{-1} lasting about 8 min is consistent with an east–west extension of 1200 km. If the flow bursts actually were related to flow vortices passing through the radar field-of-view in the way suggested above, one would expect that the direction of flow was changing. In particular, equatorward flow should be observed at the leading edge of the event and this would rotate to poleward, via westward as the vortex passed by. The north–south component of the vectors shown in Fig. 4 is directly measured by the UHF radar (which points along the magnetic meridian) and it can be seen that southward flow is absent from the onset of each event. Thus we exclude the possibility of FTE/PTE type localised convection vortices. Kelvin–Helmholtz instability and pressure pulse induced travelling twin vortices (cf. Introduction) may also be excluded using similar arguments.

It is notable that the direction of flow remained relatively unchanged (cf. Fig. 4). The first three aurora] events with a 5 min repetition period were accompanied by one major flow enhancement (cf. Fig. 2). On average the EISCAT flow voltage was ~ 20 kV, roughly 50% of the corresponding F11 transpolar values. These are all features supporting the view that the large-scale dayside polar cap flows actually had similar time variations as the EISCAT voltage. If so, there must be a transient mechanism which effectively modulates large-scale flows.

Time variations of a the convection pattern of type DE (Heppner and Maynard, 1987) may be accounted for by the Cowley and Lockwood (1992) model of flow excitation in response to pulsed reconnection. Lockwood *et al.* (1993) applied this model in order to explain the strongly enhanced flow that followed the equatorward expansion of the dayside aurora on this day. The bigger difference between the events reported here and the activity observed closer to noon by them, is that the present observations (~ 15 MLT) likely were made outside the merging gap. The model by Cowley and Lockwood (1992) predicts that the reconnection pulse erodes the dayside open/closed boundary and that when the enhanced reconnection ceases, this boundary returns poleward while other segments

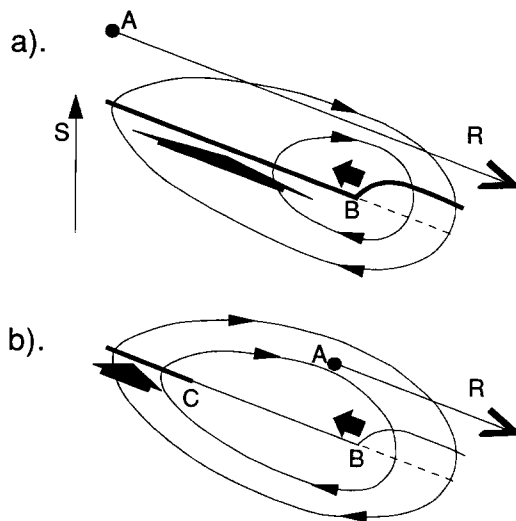


Fig. 6. Schematic illustration of possible flow onsets in the mid-afternoon sector (northern hemisphere) due to a pulse of enhanced reconnection, as predicted using the model of flow excitation by Cowley and Lockwood (1992). Diagrams are in the rest frame of a eastwardexpanding polar cap extrusion (at B), in which the radar moves to the west along the locus R, starting from A at the onset of the reconnection pulse. S denotes the direction of the southward normal to the L-shells. Case (b) differs from (a) in that a reconnection at a low (background) rate exists at the MLT of the radar at the time of the reconnection pulse. (See text for details).

of the boundary expands equatorward, allowing the ionosphere–magnetosphere system to tend towards equilibrium with the new amount open flux. This excites large-scale vortical convection. To fit observations of convection enhancements propagating away from the midday sector (Lockwood *et al.*, 1990b; Saunders *et al.*, 1992; Lockwood *et al.*, 1993) the equatorward extrusion of the polar cap is envisaged as expanding tailward. Fig. 6 demonstrates why this vortical flow, unlike that associated with the smaller-scale vortices of more localised signatures (as predicted for moving-cloud FTE models, FTEs and TCVs), need not give a southward flow as the flow enhancement expands tailward over the radar. This is important because virtually no such southward flow is observed during the events described here (see Fig. 4). Note, however, that southward flow can arise in some cases, as in the longer-lived, erosion event described by Freeman and Southwood (1988).

In Fig. 6, the extrusion of the polar cap (at B) is shown in its rest frame. Because B propagates along the open/closed boundary in the Earth's frame, in B's rest frame a radar gate (R) will move along the open/closed boundary in the Earth's frame, in B's rest frame a radar gate (R) will move along the open/closed

boundary to the west, as shown: R is at A at the time of the reconnection pulse. Thin solid lines with arrows are plasma flow stream lines, thick solid lines are adiaroic segments of the polar cap boundary (which map to magnetopause segments where no reconnection takes place) and thin solid lines are merging gaps which map to segments of the magnetopause where reconnection (at some rate) is in progress. The dashed line marks the poleward edge of the newly-opened flux produced by the reconnection pulse. Note that the L-shells run horizontally across the figure (so S is in the direction of their southward normal), the inclination of the open/closed boundary (shown here as straight for simplicity) reflecting that it is at lower invariant latitudes away from noon. In Fig. 6a, the reconnection pulse is imagined to have ceased by the time B enters the mid-afternoon sector. Behind B, the boundary, and hence the plasma around it, has a poleward boundary-normal component of V_1 ; ahead of B both have an equatorward boundary-normal component of V_2 . If the flow excited is large-scale convection, then V_2 will be much smaller in magnitude than V_1 . For example, if the half of the merging gap in the dusk convection cell is about 1000 km in length and the equatorward-moving boundary ahead of B covers 5000 km, a typical V_1 of 1 km s^{-1} will give a mean boundary-normal equatorward speed of B of $\langle V_2 \rangle = 200 \text{ m s}^{-1}$. This should be compared with the flow speeds at the onset of each event of 1 km s^{-1} , and hence the initial flows will be at an angle of about $\sin^{-1}(0.2) \approx 10^\circ$ with respect to the pre-existing open/closed boundary. As this is comparable to the tilt of the afternoon sector boundary with respect to the L-shells, the first flow produced by the event which is seen by the radar will not have a southward component but rather, as illustrated in Fig. 6a, will be westward. In addition, at the initial times when the radar is in the region where there may have been a possibility of southward flow being seen, the vortex may be much weaker than later on because the flow increase is inductively smoothed compared with the reconnection onset (as described by Lockwood *et al.*, 1993)

There are a number of other reasons why southward flow may not be present at event onset. Fig. 6b illustrates one of these which has added advantage of predicting some northward flow between events (such as can be seen between the second and third events in Fig. 4. In this example, C marks the eastward end of a merging gap along which reconnection takes place at a constant but low background rate. At the onset of the event, the radar is at A which is west of C, i.e. within this merging gap. Nearer noon, a pulse of enhanced reconnection rate (much greater than the

background rate) then produces the extrusion which expands eastward, as in Fig. 6a. As the extrusion edge (B) expands eastward, the plasma ahead of B may no longer moves equatorward (normal to the boundary) even if the boundary does. This is because the effect of the southward boundary migration is opposed by the weak poleward flow (in the boundary rest frame) produced by the low background reconnection rate. However, the equatorward migration of the adiaroic boundary to the east of C does give the large-scale flow vortex shown. Hence the flow is again westward.

In both the above cases, the flow onset is westward, with no southward component, but swings around to northward as B approaches the radar (as observed for event onsets in Fig. 4). The lack of southward flow is therefore allowed by the model large-scale flow excitation, whereas it is not for the passage of more localised vortices.

As a first order approximation the variability of the EISCAT flow voltage may be reproduced by a linear approximation as demonstrated in Fig. 2. Each event is represented by a triangle in the voltage versus time frame. The ionospheric flow associated with a single auroral event increases from a steady state background level (which is near zero in this case) to a peak value and subsequently decreases to the level of background again. The estimated rates of growth and decay of voltage are estimated to be of the same order, 4–5 kV/min. The ionospheric flows associated with one event, including a growth and decay phase, lasted about 12 min (the average base-line of the triangles in Fig. 2). Cowley and Lockwood (1992) derived a time constant for dayside flow excitation of about this value (15 min), i.e. the time taken to transfer newly-opened flux into the tail lobe. Similar values have been derived from electrical circuit analogies (Holzer and Reid, 1975; Sanchez *et al.*, 1991), “line-tying” arguments (Coroniti and Kennel, 1973) and from the EISCAT-AMPTE data on ionospheric flow response (Todd *et al.*, 1988). Given that the flow was excited for about 12 min by each event and that events repeated even 8 min on this day, we infer that, at any one time, the effects of 2 successive merging pulses contributed to dayside convection.

In this study we have demonstrated a close correlation between variations in flow voltage and auroral activity. More data on this auroral event/ion drift relationship and simultaneous IMF and solar wind/magnetosheath data are necessary before the source mechanism in the magnetospheric boundary layer can be unambiguously determined. It is quite critical for this case study that we actually do not know if the auroral transients were located on open or closed magnetic field lines. Hence, the possibility of a viscous

mechanism cannot be definitely excluded. The local time coverage of the actual auroral event sequence (~ 14 – 16 MLT) is in favour of closed field lines. However, the amplitude of the burst in transauroral voltage exceeds that seen during northward IMF and hence is unlikely to have a viscous-like origin. Independent of the actual convection driver mechanism, the strength of, the large-scale polar cap convection appears to be highly variable. High-time resolution ion flow measurements as applied in the present case is neces-

ary to explore the dynamical behaviour of the dayside high-latitude convection.

Acknowledgements—We thank the Director and the staff of the EISCAT Scientific Association for their assistance. EISCAT is supported by the research councils of the 6 member nations: France, Germany, UK, Sweden, Finland and Norway. These observations were made as a part of a GEM boundary-layer campaign. This project has been supported by grant 154/92 from 'Nansenfondet og de dermed forbundne fond'.

REFERENCES

- Coroniti F. V. and Kennel C. F. 1973 Can the ionosphere regulate magnetospheric convection?, *J. Geophys. Res.*, **78**, 2837–2851.
- Cowley S. W. H. and Lockwood M. 1992 Excitation and decay of solar wind-driven flows in the magnetosphere–ionosphere system, *Ann. Geophys.*, **10**, 103–115.
- Doyle M. A. and Burke W. J. 1983 S3-2 measurements of the polar cap potential, *J. Geophys. Res.*, **88**, 9125–9133.
- Freeman M. P. and Southwood D. J. 1988 The effect of magnetospheric erosion on mid-and high-latitude ionospheric flows, *Planet. Space Sci.*, **36**, 507.
- Friis-Christensen E., McHenry M. A., Clauer C. R. and Vennestrøm S. 1988 Ionospheric travelling convection vortices observed near the polar cleft: A triggered response to sudden changes in the solar wind, *Geophys. Res. Lett.*, **15**, 253–256.
- Heppner J. P. and Maynard N. C. 1987 Empirical high-latitude electric field models, *J. Geophys. Res.*, **92**, 4467–4490.
- Holzer T. E. and Reid G. C. 1975 The response of the dayside magnetosphere ionosphere system to time-varying field line reconnection at the magnetopause. I. Theoretical Model, *J. Geophys. Res.*, **80**, 2041–2049.
- Kivelson M. G. and Southwood D. J. 1990 Ionospheric travelling vortex generation by solar wind buffeting of the magnetosphere, *J. Geophys. Res.*, **96**, 1661–1667.
- Lemaire J., Rycroft M. J. and Roth M. 1979 Control of impulsive penetration of solar wind irregularities into the magnetosphere by the interplanetary magnetic field direction, *Planet. Space Sci.*, **27**, 47–57.
- Lockwood M., Sandholt P. E., Cowley S. W. H. and Ogoti T. 1989 Interplanetary magnetic field control of dayside auroral activity and the transfer of momentum across the dayside magnetopause, *Planet. Space Sci.*, **37**, 1347.
- Lockwood M., Sandholt P. E., Farmer A. D., Cowley S. W. H., Lybekk B. and Davda V. N. 1990a Auroral and plasma flow transients at magnetic noon, *Planet. Space Sci.*, **38**, 973–993.
- Lockwood M., Cowley S. W. H. and Freeman M. P. 1990b The excitation of plasma convection in the and high-latitude ionosphere, *J. Geophys. Res.*, **95**, 7961–7972.
- Lockwood M., Moen J., Cowley S. W. H., Farmer A. D., Løvhaug U. P., Lühr H. and Davda V. N. 1993 Variability of dayside convection and motions of the cusp/cleft aurora, *Geophys. Res. Lett.*, **20**, 1011–1014.
- Ma Z. W., Hawkins J. G. and Lee L. C. 1991 A simulation study of impulsive penetration of solar wind irregularities into the magnetosphere at the dayside magnetopause, *J. Geophys. Res.*, **15**, 751–15, 765.
- McHenry M. A., Clauer C. R., Friis-Christensen E., Newell P. T. and Kelly J. D. 1990a Ground observations of magnetospheric boundary layer phenomena, *J. Geophys. Res.*, **95**, 14995–15005.
- McHenry M. A., Clauer C. R. and Friis-Christensen E. 1990b Relationship of solar wind parameters to continuous, dayside, high latitude travelling ionospheric vortices, *J. Geophys. Res.*, **95**, 15007–15022.
- Newell P. T. and Sibeck D. G. 1993 B_y fluctuations in the magnetosheath and azimuthal flow velocity transients in the dayside ionosphere, *Geophys. Res. Lett.*, **20**, 1719–1722.
- Russell C. T. and Elphic R. C. 1979 ISEE observations of flux transfer events at the dayside magnetopause, *Geophys. Res. Lett.*, **6**, 33–36.

- Sanchez E. R., Siscoe G. L. and Meng C.-I 1991 Inductive attenuation of the transpolar voltage, *Geophys. Res. Lett.*, **18**, 1173–1176.
- Sandholt P. E., Deehr C. S., Egeland A., Lybekk B., Viereck R. and Romick G. J. 1986 Signatures in the dayside aurora of plasma transfer from the magnetosheath, *J. Geophys. Res.*, **91**, 10,063–10,079.
- Sandholt P. E., Lybekk B., Egeland A., Nakamura R. and Oguti T. 1989 Midday auroral breakup, *J. Geomagn. Geoelectr.*, **41**, 371.
- Sandholt, P. E., Moen J., Rudland A., Opsvik D., Denig W. F. and T. Hansen 1993 Auroral event sequences at the dayside polar cap boundary for positive and negative IMF B_y , *J. Geophys. Res.*, **98**, 7737–7755.
- Saunders M. A., Freeman M. P., Southwood D. J., Cowley S. W. H, Lockwood M., Samson J. C., Farrugia C. J. and Hughes T. J. 1992 Dayside ionospheric convection changes in response to long-period interplanetary magnetic field oscillations: Determination of ionospheric phase velocity, *J. Geophys. Res.*, **97**, 19,373–19,380.
- Sibeck D. G. 1990 A model for transient magnetospheric response to sudden solar wind dynamic pressure variations, *J. Geophys. Res.*, **95**, 3755–3771.
- Siscoe G. L. and Huang T. S. 1985 Polar cap inflation and deflation, *Geophys. Res. Lett.*, **90**, 543–547.
- Southwood D. J. 1987 The ionospheric signature of flux transfer events, *J. Geophys. Res.*, **92**, 3207–3213.
- Todd H., Cowley S. W. H., Lockwood M., Willis D. M. and Lühr H. 1988 Response time of the high-latitude dayside ionosphere to sudden changes in the north–south component of the IMF, *Planet. Space Sci.*, 1415–1428.
- Wei C. Q. and Lee L. C. 1990 Ground magnetic signatures of moving elongated plasma clouds, *J. Geophys. Res.*, **95**, 2405–2418.
- Wei C. Q. and Lee L. C. 1993 Coupling of magnetopause-boundary layer to the polar ionosphere, *J. Geophys. Res.*, **98**, 5707–5725.
- Woch J. and Lundin R. 1992 Signatures of transient boundary layer processes observed with Viking, *J. Geophys. Res.*, **97**, 1431–1447.